Phys Chem Minerals (1997) 24: 274–280

ORIGINAL PAPER

P. Comodi · P.F. Zanazzi

Pressure dependence of structural parameters of paragonite

Received April 10, 1996 / Revised, accepted September 27, 1996

Abstract The compressibility and structure of a $2M_1$ paragonite with composition $[Na_{0.88}K_{0.10}Ca_{0.01}Ba_{0.01}][Al_{1.97}Ti_{0.007}Fe_{0.01}Mn_{0.002}Mg_{0.006}]Si_{3.01}Al_{0.99}O_{10}OH_2$ were determined at pressures between 1 bar and 41 kbar, by single crystal X-ray diffraction using a Merrill-Bassett diamond anvil cell.

Compressibility turned out to be largely anisotropic, linear compressibility coefficients parallel to the unit cell edges being $\beta_a=3.5(1)\cdot10^{-4}$, $\beta_b=3.6(1)\cdot10^{-4}$, $\beta_c=8.3(3)\cdot10^{-4}$ kbar^{-1} ($\beta_a:\beta_b\cdot\beta_c=1:1028:2.371$). The isothermal bulk modulus, calculated as the reciprocal of the mean compressibility of the cell volume, was 650(20) kbar.

The main features of the deformation mechanism resulting from structural refinements at pressures of 0.5, 25.4, 40.5 kbar were:

– variation in sheet thickness, showing that compression of the *c* parameter was mainly due to the interlayer thickness reduction from 3.07 Å at 0.5 kbar to 2.81 Å at 40.5 kbar;

– the compressibility of octahedra was greater than that of tetrahedra, the dimensional misfit between tetrahedral and octahedral sheets increased with *P*, so that tetrahedral rotation angel α increased from 15° at 0.5 kbar to 21.6° at 40.5 kbar;

– the basal surface corrugation (Δz) of the tetrahedral layer, due to the different dimensions of M1 and M2 octahedra and to the octahedral distortion, decreased with *P* ($\Delta z=0.19$ and 0.12 Å at 0.5 and 40.5 kbar respectively).

Comparison of the new data on paragonite with those of a K-muscovite and a Na-rich muscovite (Comodi and Zanazzi 1995) revealed a clear trend toward decreasing of compressibility when Na substitutes for K atoms in the interlayer sites.

Paola Comodi · Pier Francesco Zanazzi (✉)
Dipartimento di Scienze della Terra, Università di Perugia,
Piazza Università, I-06100 Perugia, Italy
Fax: +39-75-5853203; e-mail: Zanazzi@unipg.it

Introduction

Paragonite, $NaAl_2Si_3AlO_{10}(OH)_2$, is a dioctahedral mica which is the Na analogue of muscovite. It occurs commonly in many blueschist and eclogites facies metamorphic rocks. It also occurs in metapelitic rocks from the greenschist to sillimanite zone of amphibole facies, primarily if the rocks are more Al-rich than the typical metapelite (Guidotti 1984).

The large asymmetric solvus between Paragonite (Pg) and Muscovite (Ms) has long been known (see Guidotti et al. 1994 for early references). Moreover, there have been many attempts to use the partitioning of Na and K between coexisting Ms ang Pg as a geothermometer (see Blencoe et al. 1994 for a recent discussion thereof). Inasmuch as the exact shape of the solvus and how it changes with pressure is not yet well known, thermometric estimates are often inconsistent with corresponding temperatures derived from alternative methods. The molar volumes of the terms along Ms-Pg join and how they change with pressure must be known before a more accurate phase diagram can be drawn. The aim of this work is to contribute to the knowledge of the molar volume of paragonite and its variation with *P* through compressibility measurements on single crystals. Structural refinements with high-pressure data can also show the deformation mechanism of the Pg structure with *P*.

Comparison of the data presented here with compressibility data from a Ms (K-ms) and a Na-rich Ms (Na-ms) (Comodi and Zanazzi 1995), allows evaluation of the role of Na↔K substitution in the baric behaviour of white dioctahedral micas.

Experimental

Because Pg usually occurs as fine-grained aggregates, it was very difficult to find a good single crystal suitable for study on a four-circle automated diffractometer. A good sample of the Pg $2M_1$ polytype was found in a specimen from the Western Alps (sample (Al-433 obtained from M. Frey), and kindly provided to us by C.V.

Guidotti. The sample, with formula $[Na_{0.88}K_{0.10}Ca_{0..01}Ba_{0.01}][Al_{1.97}Ti_{0.007}Fe_{0.01}Mn_{0.02}Mg_{0.006}]Si_{3.01}Al_{0.99}O_{10}OH_2$, had a Na/Na+K ratio of 0.90, intermediate between the value of 0.96 of the sample refined by Lin and Bailey (1984) [LBpg], and the value of 0.85 of the sample studied by Burnham and Radoslovich (1964) [BRpg].

Diffraction data were collected at ambient conditions on a four-circle Philips PW1100 diffractometer, from a crystal with dimensions $0.12\times0.10\times0.06$ mm^3, using graphite monochromatized MoKα radiation ($\lambda=0.7107$ Å); ω scans with scan width 3.5° and speed in the range 0.06–0.12° s^{-1} were employed. 2544 integrated intensities from two equivalent sets with indices $\pm hkl$ and $\pm h\bar{k}l$ (up to 35° θ) were collected for structural refinement (Table 1). An empirical absorption correction based on the method of North et al. (1968) was applied: transmission factors were in the range 1.0–0.87. After merging of equivalent reflections ($R_{eq}=2.4\%$), a total of 1043 independent reflections was obtained, with intensities higher than 3σ. Anisotropic refinement in space group $C2/m$ was carried out using the SHELX-76 program (Sheldrick 1976). The theoretically vacant M1 site was considered partially occupied by Mg because the refinement showed that about 0.2 electrons were present. In the late stages of refinement, one peak in the Fourier difference map was assigned to the hydrogen atom of the

Table 1 Refinement details

P(kbar)	0.001	0.5	25.4	40.5
No. measured reflections	2544	822	746	689
No. independent reflections	1043	243	219	187
No. variables	94	41	41	41
R_{eq}*	2.4	4.1	6.4	5.3
R**	2.1	6.1	7.0	6.5

* $R_{eq}=\sum_h\sum_j||F_h|-|F_{hj}||/\sum_h\sum_j|F_{hj}|$

** $R=\sum||F_{obs}|-|F_{calc}|/\sum|F_{obs}|$

Table 2 Fractional atomic coordinates and thermal parameters (Å^2). For H*P* refinements and H atom the isotropic thermal parameters are given. For each entry the four values refer to 0.001, 0.5, 25.4, 40.5 kbar refinement respectively

Atom	*x*	*y*	*z*	U11/Uis	U22	U33	U23	U13	U12
T1	0.9555(1)	0.4284(1)	0.1043(1)	0.0092(2)	0.0094(2)	0.0149(2)	0.0001(1)	0.0007(1)	0.0002(1)
	0.9568(8)	0.4288(4)	0.1411(7)	0.0063(9)					
	0.9613(8)	0.4271(5)	0.1430(1)	0.004(1)					
	0.963(1)	0.4269(6)	0.142(1)	0.004(1)					
T2	0.4423(1)	0.2575(1)	0.1403(1)	0.0091(2)	0.0090(2)	0.0145(2)	0.0002(1)	0.0001(1)	0.0003(1)
	0.4426(7)	0.2578(4)	0.1399(7)	0.0067(9)					
	0.4490(8)	0.2563(5)	0.1412(8)	0.007(1)					
	0.450(1)	0.2566(6)	0.141(1)	0.007(1)					
M2	0.2501(1)	0.0834(1)	0.0000(1)	0.0076(2)	0.0079(2)	0.0135(2)	0.0002(1)	0.0003(2)	−0.0005(1)
	0.2494(8)	0.0831(4)	0.0007(6)	0.0048(8)					
	0.2476(9)	0.0827(5)	0.0011(8)	0.005(1)					
	0.251(1)	0.0829(6)	−0.0004(9)	0.003(1)					
Na	0	0.0946(1)	1/4	0.0293(7)	0.0365(8)	0.0295(7)	0	0.0092(4)	0
	0	0.094(1)	1/4	0.032(3)					
	0	0.095(1)	1/4	0.021(3)					
	0	0.095(1)	1/4	0.017(3)					
O1	0.9581(2)	0.4439(1)	0.0553(1)	0.0095(5)	0.0107(5)	0.0150(5)	0.0016(4)	0.0002(4)	0.0015(4)
	0.959(2)	0.445(1)	0.056(2)	0.004(2)					
	0.959(2)	0.440(1)	0.054(2)	0.009(3)					
	0.960(2)	0.439(1)	0.051(3)	0.000(3)					
O2	0.3807(2)	0.2517(1)	0.0554(1)	0.0116(5)	0.0077(5)	0.0149(5)	0.0003(3)	−0.0010(4)	0.0003(4)
	0.382(2)	0.251(1)	0.055(2)	0.007(2)					
	0.385(2)	0.252(1)	0.053(2)	0.007(2)					
	0.389(2)	0.251(2)	0.054(2)	0.007(3)					
O3	0.3785(2)	0.0918(1)	0.1737(1)	0.0190(6)	0.0126(5)	0.0175(2)	0.0009(4)	0.0016(4)	0.007(4)
	0.375(2)	0.092(1)	0.174(1)	0.015(2)					
	0.373(2)	0.092(1)	0.178(2)	0.012(3)					
	0.372(2)	0.090(2)	0.175(2)	0.007(9)					
O4	0.7513(2)	0.2968(1)	0.1622(1)	0.0154(6)	0.0173(5)	0.0200(5)	0.0017(4)	−0.0008(4)	−0.024(4)
	0.751(2)	0.297(1)	0.164(1)	0.013(2)					
	0.762(2)	0.290(1)	0.169(2)	0.009(3)					
	0.765(3)	0.287(1)	0.170(2)	0.009(4)					
O5	0.2505(2)	0.3811(1)	0.1743(1)	0.0148(6)	0.0165(5)	0.0176(5)	−0.0018(4)	−0.0004(4)	0.0023(4)
	0.250(2)	0.381(1)	0.174(1)	0.013(2)					
	0.262(2)	0.384(1)	0.179(2)	0.013(3)					
	0.264(3)	0.385(1)	0.179(2)	0.014(4)					
OH	0.9527(2)	0.0626(1)	0.0512(1)	0.0101(5)	0.0110(5)	0.0178(5)	−0.033(4)	0.0017(4)	−0.0020(4)
	0.954(2)	0.064(1)	0.051(1)	0.009(2)					
	0.955(2)	0.063(1)	0.052(2)	0.003(3)					
	0.953(2)	0.066(1)	0.055(2)	0.007(3)					
H	0.373(8)	0.636(4)	0.071(2)	0.08(1)					

hydroxyl group. Further refinement cycles, including hydrogen atom contribution, improved the agreement index and resulted in a final *R* of 2.1% for 94 parameters. The neutral atomic scattering factor values from the International Tables for X-ray Crystallography (1974) were employed. Mixed curves computed on the basis of chemical analysis were used for interlayer and tetrahedral sites.

Final atomic coordinates and thermal parameters are listed in Table 2; observed and calculated structure factors may be obtained from the authors on request.

A Merrill-Bassett diamond anvil cell (DAC) with 1/8 carat diamonds was used for the high-pressure study. A Sm^{2+}:BaFCl powder for pressure calibration (Comodi and Zanazzi 1993) and a 16:3:1 methanol:ethanol:water mixture as pressure-transmitting medium were introduced into the DAC together with the sample. Pressure was monitored by measuring the wavelength shift of the Sm^{2+} line excited by a 100-mw argon laser and detected by a 100-cm Jarrell-Ash optical spectrometer. The precision of the pressure measurements was 0.5 kbar. Steel foil 250 μm thick, with a hole of 300 μm diameter, was used as gasket material. The lattice parameters of two crystals, selected from the same sample and independently mounted in the DAC, were determined at various pressures between 0.001 and 41 kbar (Table 3) by applying the least-squares method to the Bragg angles of about 30 accurately centered reflections in the range 10–30° 2θ.

The intensity data of paragonite were collected at 25.4 and 40.5 kbar up to 35° θ, adopting non-bisecting geometry (Denner et al. 1978) and 4.0° ω scans; data were corrected for pressure-cell absorption by an experimental attenuation curve (Finger and King 1978). Since systematic errors may be introduced by comparison of refinement results obtained by reflections measured at room conditions belonging to the whole reciprocal lattice, with results obtained by reflections measured within the DAC, from a limited part of the reciprocal space, the same set of intensity data was collected at 0.5 kbar from the same crystal and using the same procedure.

Intensity data were analysed with a digital procedure (Comodi et al. 1994), visually inspected to eliminate errors due to the overlap of diffraction effects from various parts of the diamond cell or to shadowing by the gasket, and merged to form an independent data set.

The structure was refined in space group *C*2/*m*, with individual isotropic atomic displacement parameters, using the SHELX-76 program. Final *R* values were 6.1, 7.0 and 6.5% for 243, 219 and 187 independent observed reflections and 41 parameters, respectively for refinements at 0.5, 25.4 and 40.5 kbar. Details of refinements are listed in Table 1; final fractional atomic positions and thermal parameters are presented in Table 2.

Table 3 Lattice parameters and volumes of paragonite *vs* pressure. Asterisks indicate the measurements on the second sample

P (kbar)	*a* (Å)	*b* (Å)	*c* (Å)	β (°)	*V* (Å³)
0.001	5.135(1)	8.906(1)	19.384(4)	94.6(1)	883.6(4)
0.001*	5.134(1)	8.907(1)	19.360(4)	94.5(1)	882.6(4)
0.5*	5.134(3)	8.906(5)	19.32(1)	94.5(2)	881(1)
3.7	5.129(2)	8.876(3)	19.324(8)	95.5(2)	875.7(8)
5.8*	5.127(3)	8.890(6)	19.24(2)	94.6(2)	874(1)
7.7	5.120(4)	8.878(4)	19.22(1)	94.8(2)	870.6(9)
13.2	5.111(2)	8.864(3)	19.11(2)	95.0(2)	862(1)
14.0*	5.108(2)	8.852(6)	19.06(1)	94.7(2)	859(1)
19.0	5.099(2)	8.842(4)	19.03(2)	95.0(2)	855(1)
25.4*	5.082(2)	8.813(5)	18.91(1)	94.7(2)	844(1)
27.0	5.086(2)	8.818(3)	18.90(2)	95.1(2)	844(1)
29.0	5.085(2)	8.816(3)	18.90(2)	95.1(2)	844(1)
31.0*	5.072(3)	8.802(5)	18.85(2)	94.6(2)	839(1)
34.4*	5.071(2)	8.793(3)	18.77(2)	94.8(2)	834(1)
34.8	5.076(3)	8.801(4)	18.82(1)	95.1(2)	837(1)
37.8*	5.061(2)	8.780(3)	18.74(2)	94.8(2)	830(1)
37.9	5.072(2)	8.780(3)	18.82(2)	95.1(2)	835(1)
40.5*	5.062(2)	8.769(3)	18.64(2)	95.2(2)	824(1)

Results at ambient conditions

The general features of the Pg structure agree with those described by Lin and Bailey (1984) and Burnham and Radoslovich (1964). Some relevant structural parameters, such as bond lengths and polyhedral volumes are given in Table 4; tetrahedral, octahedral and interlayer thicknesses, and some distortion parameters, are given in Table 5.

Tetrahedral and octahedral bond lengths are equal within the σ to those reported for LBpg and BRpg. The bond lengths concerning the interlayer cation are more similar to those of potassian paragonite BRpg. The structural parameters which are functions of the K content were, as expected, intermediate between the values found in LBpg and those in BRpg. For example tetrahedral rotation α computed with the method of Güven (1971) is 16.0°, and is to be compared with 16.2° in LBpg and 15.9° in BRpg.

The hydrogen position determined by our X-ray refinement showed that the O−H bond was inclined with respect to the *c** direction. The Na−H−O angle was about 108°. Actually, in dioctahedral micas, the proton is

Table 4 Bond lengths (Å) and polyhedral volumes (Å³) of paragonite at different pressures

P (kbar)	0.001	0.5	25.4	40.5
T1−O1	1.654(1)	1.65(3)	1.69(3)	1.69(4)
T1−O4	1.651(1)	1.66(1)	1.68(2)	1.70(2)
T1−O5	1.658(1)	1.64(1)	1.66(2)	1.66(2)
T1−O3	1.653(1)	1.65(1)	1.67(1)	1.64(1)
⟨T1−O⟩	1.654	1.65	1.68	1.67
VT1	2.320(4)	2.30(5)	2.41(9)	2.39(9)
T2−O2	1.652(1)	1.64(2)	1.67(3)	1.64(4)
T2−O3	1.655(1)	1.66(2)	1.67(2)	1.66(2)
T2–O4	1.647(1)	1.65(1)	1.66(1)	1.66(1)
T2−O5	1.649(1)	1.64(1)	1.67(2)	1.66(2)
⟨T2−O⟩	1.651	1.65	1.67	1.65
VT2	2.306(4)	2.30(6)	2.37(9)	2.31(9)
M1−O1 (×2)	2.257(1)	2.27(2)	2.19(2)	2.15(2)
M1–O2 (×2)	2.253(1)	2.24(2)	2.18(2)	2.15(2)
M1−OH (×2)	2.166(1)	2.16(2)	2.14(2)	2.13(2)
⟨M1−O⟩	2.225	2.22	2.17	2.14
VM1	13.94(2)	13.9(4)	12.9(4)	12.4(4)
M2−O1	1.911(1)	1.90(2)	1.88(2)	1.86(2)
M2−O2	1.932(1)	1.92(2)	1.89(2)	1.89(2)
M2−O2′	1.910(1)	1.92(2)	1.88(2)	1.87(2)
M2−OH	1.895(1)	1.87(2)	1.84(2)	1.91(2)
M2−OH′	1.896(1)	1.90(2)	1.89(2)	1.91(2)
M2−O1′	1.927(1)	1.94(2)	1.89(2)	1.82(2)
⟨M2−O⟩	1.912	1.91	1.88	1.88
VM2	9.10(1)	9.1(2)	8.6(2)	8.6(2)
Na−O3 (×2)	2.534(1)	2.52(2)	2.42(2)	2.44(2)
Na−O4 (×2)	2.724(1)	2.71(2)	2.54(2)	2.48(2)
Na−O5 (×2)	2.667(1)	2.67(2)	2.54(2)	2.51(2)
$\langle NA-O\rangle_{inner}$	2.642	2.63	2.50	2.48
V_{Na}	26.46(3)	24.2(5)	20.7(5)	20.2(5)
Na−O3′ (×2)	3.409(1)	3.42(2)	3.36(2)	3.36(2)
Na−O4′ (×2)	3.456(1)	3.43(2)	3.42(2)	3.41(2)
Na−O5* (×2)	3.258(1)	3.26(2)	3.21(2)	3.21(2)
$\langle NA-O\rangle_{outer}$	3.374	3.37	3.33	3.33

Note: the suffix inner or outer refers to the six shorter or longer Na−O distances respectively

Table 5 Some relevant structural parameters of paragonite at different pressures

P (kbar)	0.001	0.5	25.4	40.5
tetrahedral thickness (Å)	2.243(4)	2.24(5)	2.31(5)	2.25(5)
octahedral thickness (Å)	2.085(4)	2.08(5)	2.00(5)	1.98(5)
interlayer thickness (Å)	3.090(4)	3.07(5)	2.80(5)	2.81(5)
T−O−T thickness (Å)	6.571(4)	6.56(5)	6.62(5)	6.48(5)
Δ (Å)*	0.73	0.74	0.89	0.92
α (deg)**	14.9	15.0	20.3	21.6
Δz (Å)***	0.23	0.19	0.18	0.12

* $\Delta=[2\sqrt{3}e_b-3\sqrt{2}d_o]$ where e_b=the mean of all basal tetrahedral edge lengths and d_o=the mean of all M−O, OH octahedral bond lengths
** $\alpha=[35.44\Delta-11.09]$
*** $\Delta z=[(z_{O5}+z_{O3})/2-z_{O4}]c\sin\beta$

repulsed from the interlayer cation and the O−H bond points toward the vacant M1 site, as shown by Rothbauer (1971).

Comparison of this refinement with that of muscovite (Comodi and Zanazzi 1995) allowed the main structural variations produced by Na↔K substitution in the structure of dioctahedral mica to be analysed, as follows:
– as pointed out by Radoslovich (1963), minimization of the geometric misfit between tetrahedral and octahedral layers through the tetrahedral rotation mechanism is partially hindered in muscovite because of the dimension of the K cation. Since the interlayer cation size is smaller in Pg than in Ms, the dimensional misfit between octahedral and tetrahedral sheets can be minimized through more pronounced tetrahedral rotation. Therefore the α angle assumes a higher value in Pg (14.9°) than in Ms (10.3°); these values were calculated with the equation proposed by Toraya (1981);
– as a consequence, lattice parameters *a* and *b*, respectively 5.135 and 8.907 Å, were approximately 1% smaller than those of Ms (5.195 and 9.020 Å respectively), although the two micas had about the same T−O−T composition;
– in the interlayer cavity, the difference between the means of the six largest (3.375 Å) and six shortest (2.642 Å) cation-anion distances was 0.733 Å. In Ms, the same difference was 0.509 Å. Therefore, in Pg the coordination of Na may be considered sixfold, fitting an irregular octahedron. Distortion of this octahedron could be estimated by the difference between the longest (Na−O4) and shortest (Na−O3) bond lengths, which was 0.190 Å.

Results at high pressure

Compressibility

Figure 1 shows the variations in lattice parameters of paragonite with pressure. Lattice constants and cell-volume values at various pressures are listed in Table 3. As indicated by the very high correlation coefficients of the linear regression, all parameters decreased linearly in the *P* range investigated. Linear compressibility coefficients parallel to unit cell edges were $\beta_a=3.5(1)\cdot10^{-4}$, $\beta_b=3.6(1)\cdot10^{-4}$, $\beta_c=8.3(3)\cdot10^{-4}$ kbar^{-1}, whereas the β angle remained unchanged. As already found in other phyllosilicates, the compressibility of Pg was largely anisotropic, the compressibility of parameters *a* and *b* being less than half that of parameter *c* ($\beta_a:\beta_b:\beta_c=1:1.028:2.371$).

From the unit cell data, volume variations with *P* can be described by the equation $V/V_0=1-0.00153(4)\,P$, with *P* in kbar.

The isothermal bulk modulus, calculated as the reciprocal of the mean compressibility of the cell volume, was 655(20) kbar. This value is to be compared with those of 560(15) and 600(20) kbar, recalculated with the same method respectively for K-muscovite and Na-rich muscovite from the data of Comodi and Zanazzi (1995).

Bulk modulus K_0 and its pressure derivative K_0', determined by fitting the unit-cell volumes with a third-order Birch-Murnaghan equation of state using the BIRCH program (Ross and Webb 1990), were 530(35) kbar and 5.5(2.5). Agreement with the K_0 value from the least-squares regression line through the V/V_0 values *vs P* was not very good and the value for K_0' was only approximate: this may have been due to the relatively small pressure range investigated.

Structural variations under high pressure

Bond lengths and some relevant structural parameters under high pressure are given in Tables 4 and 5.

An increase in Si−O bond lengths is generally observed in the structures of silicates refined under moderate pressure. This is the inverse to their behaviour at high temperatures, when a decrease is observed. This high temperature effect has been explaind as due to a greater thermal displacement of atoms, leading to a shorter mean separation between the centroids of electronic density. The apparent shorter bond length should be corrected for thermal motion according to various models (riding motion, correlated, uncorrelated or anticorrelated motion, Hazen and Finger 1982; Busing and Levy 1964), although unfortunately the actual model is unknown and the correction is therefore necessarily approximate. Another explanation for the effect is the need for electrostatic balance of tetrahedral oxygens which, owing to polyhedral expansion, are farther from other cations (Catti et al. 1988). These effects appear to be reversed in the case of structures under high pressure, which leads to a slight increase in tetrahedral bond lengths and volumes.

For Pg, similar effects of *P* on T−O distances were detected in the *P* range investigated. Single tetrahedral T−O bond length variations were positive or negative, although they were not fully significant on the basis of their σ's. On the whole, tetrahedral volume slightly increased. Tetrahedral thickness also apparently increased from 2.24(5) to 2.25(5)Å (see Table 5), but this effect may be explained as partially due to tetrahedral tilting out of the (001) plane.

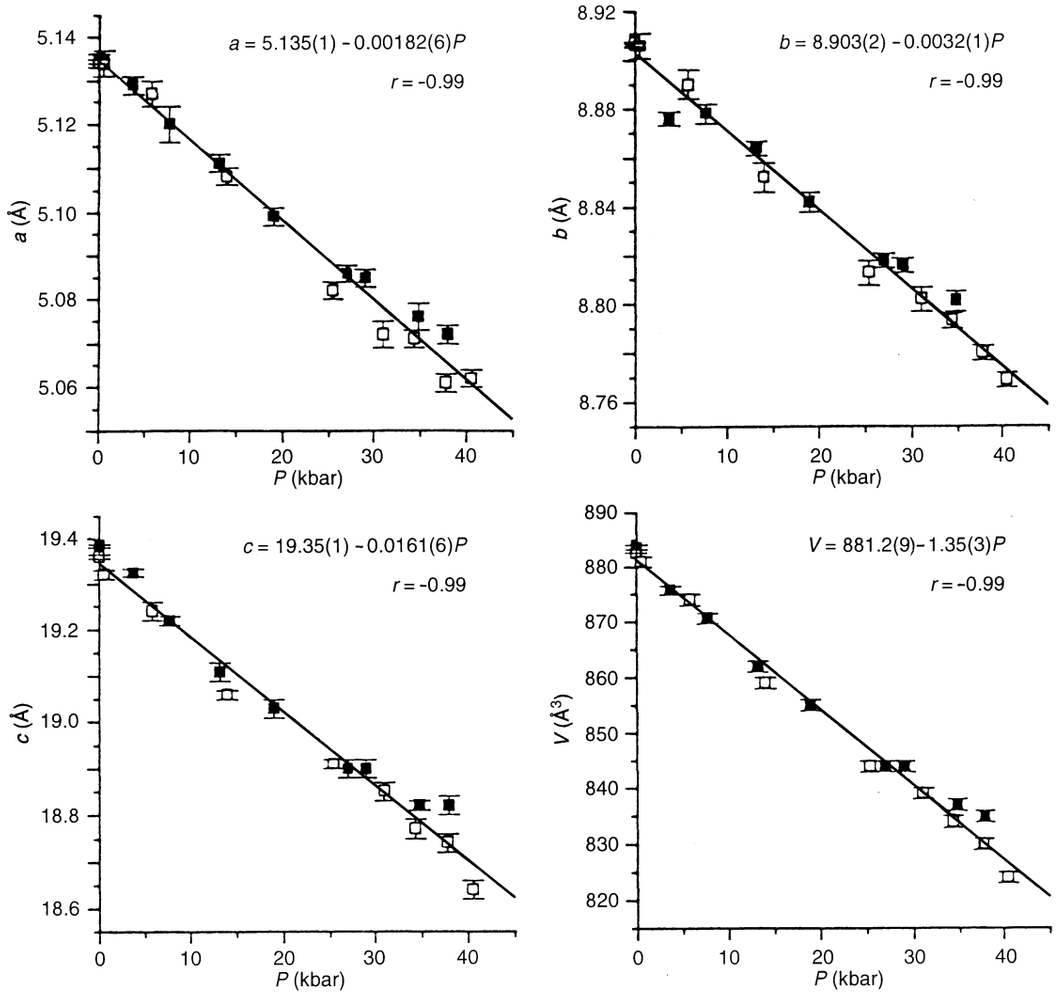

Fig. 1 Variation in lattice parameters and cell volume of paragonite. Closed and open squares refer to the two samples examined

In the nominally vacant M1 site, the mean M1−O distances decreased by 3.6%, from 2.22 to 2.14 Å, when pressure increased from 0.5 to 40.5 kbar. The polyhedral bulk modulus was 360(100)kbar. The mean M2−O changed from 1.91 to 1.87 Å and the volume from 9.1(2) to 8.6(2) Å^3, with a bulk modulus of 700(200) kbar. Octahedral thickness changed from 2.08(5) to 1.98(5) Å.

The different compressibility of tetrahedral and octahedral layers caused an increase in the dimensional misfit with *P*. In order for this misfit to be released, two mechanisms were required: rotation of tetrahedra within the plane, with an increase in α rotation angle which changed from 1.50° to 21.6°; and tilting in elevation, with a reduction of corrugation parameter Δz, as defined by Güven (1971). This value changed from 0.19(5) to 0.12(5) Å and may be partially responsible for the increased thickness of the tetrahedral layer.

Owing to the mutually compensating variations in the thicknesses of tetrahedral and octahedral layers, on the whole the thickness of the 2:1 T−O−T layer changed only slightly with increasing *P*. Its value changed from 6.56(5) Å at 0.5 kbar to 6.48(5) Å at 40.5 kbar.

The greatest changes with *P* were found in the interlayer region, where the mean Na[6]−O distance decreased from 2.63 Å at 0.5 kbar to 2.48 Å at 40.5 kbar. The volume of the Na polyhedron changed from 24.2(5) to 20.2(5) Å^3, with a polyhedral bulk modulus of 220(30) kbar. The increase in *P* had fewer effects on the outer Na−O distances, which changed from 3.37 to 3.33 Å. The thickness of the interlayer region changed from 3.07(5) Å at 0.5 kbar to 2.81(5) Å at 40.5 kbar, representing the greatest deformation in paragonite under pressure. In fact, the compressibility of the interlayer region was about seven times that of the T–O−T layer. The decrease in the cell volume of paragonite under pressure was mainly ascribable to the change in volume of the interlayer region.

Effect of Na↔K substitution on behaviour under pressure

To evaluate the effect of Na↔K substitution in dioctahedral micas, these new data can be compared with the compressibility data of the two muscovites with different Na content determined by Comodi and Zanazzi (1995). Figure 2 reports the bulk modulus data *vs* the Na/Na+K ratio. It is evident that the bulk modulus increases as the Na/Na+K ratio increases in the interlayer site. Moreover, the difference in bulk modulus is entirely due to greater compressibility along the *c* axis as the K/Na ratio increases.

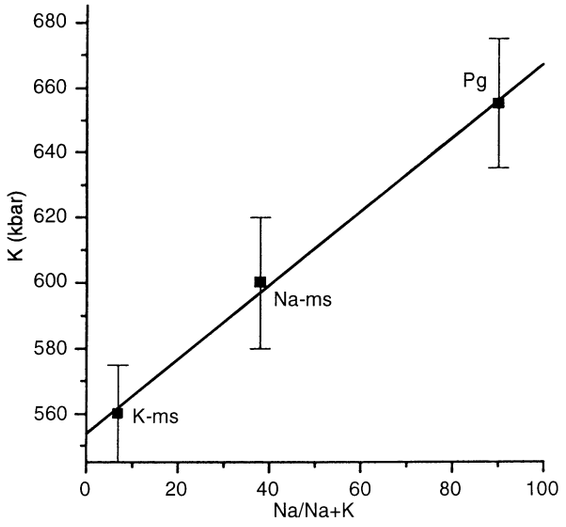

Fig. 2 Bulk moduli (kbar) *vs* Na/Na+K ratio for K-ms, Na-ms and Pg

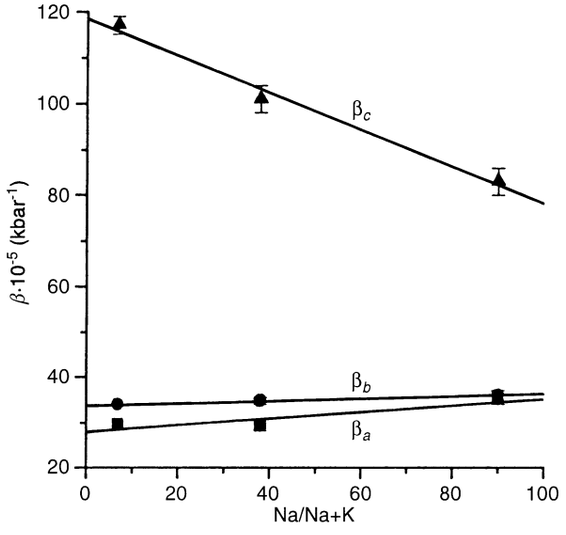

Fig. 3 Compressibility coefficients of lattice parameters *vs* Na/Na+K ratio for K-ms, Na-ms and Pg

For additional information on how the compressibility of lattice parameters changes in the three micas, Fig. 3 plots their compressibility coefficients *vs* the Na/Na+K ratio. Whereas β_a and β_b are more or less independent of interlayer content, β_c decreases linearly with increasing Na/Na+K ratio. The absence of significant phengitic component in the samples shows that the observed difference in compressibility is due solely to Na−K substitution. The smaller compressibility observed as the Na content increases is explained by stronger repulsion of the basal oxygen sheets on both sides of the interlayer ions, due to shorter *c*sin β and greater α rotation.

Conclusions

Observations on compressibility and the structural variation induced by pressure on paragonite-muscovite solid solutions enable a number of meaningful comments to be made:

1) dioctahedral micas on the Pg−Ms join, like those of all other phyllosilicates, are markedly more compressible in the [001] direction than in the *a* or *b* directions;

2) the differences in bulk modulus between the samples along the Pg−Ms join are mainly due to the difference in compressibility of the interlayer region. Compressibility is inversely related to the Na/Na+K ratio;

3) the smaller compressibility observed as Na increases is explained by stronger repulsion of the basal oxygen sheets on both sides of the interlayer ions, due to shorter *c*sin β and greater β rotation;

4) the octahedral sheet is slightly more compressible than the tetrahedral sheet. Therefore, as *P* increases, tetrahedral rotation also increases, allowing highly-charged cations to come into closer proximity, while bond lengths between basal oxygens and alkali atoms decrease. Regarding the implications which these geometric effects of *P* may have on the stability of the mica structure, the apparently destabilizing effects can be minimized by substituting Fe and Mg for Al in octahedral sites and Si for Al in tetrahedral sites: a smaller tetrahedral rotation yields a larger interlayer site, more suitable for the entry of K. This has in fact been documented from observations on natural occurrences of phengitic muscovite in high-pressure environments and may explain the relationships between phengitization and pressure (Guidotti et al. 1994);

5) the new high-*P* data presented here show that compressibility is inversely related to the Na content of the mica. This implies that the solvus and both magnitude and shape of V_{ex} of Na−K mixing might change with *P* along the Pg−Ms join. Since Pg is less compressible than Ms, an increase in *P* affects the Na limb of the solvus with respect to the K side of the solid solution to a lesser extent, in agreement with chemical data for natural Pg−Ms pairs from parageneses of various pressures (Guidotti et al. 1994). The high compressibility of Pg−Ms micas can have relevant effects on the thermody-

namic parameters of metamorphic reactions involving these minerals at different pressure.

Acknowledgements We wish to thank Prof. Charles V. Guidotti for the paragonite sample and analytical data, and for very useful discussions and comments. Financial support was provided by MURST (40% and 60% funds) and CNR (grant no. 95.00372.CT05).

References

Blencoe JG, Guidotti CV, Sassi FP (1994) The paragonite-muscovite solvus: II. Numerical geothermometers for natural, quasibinary paragonite-muscovite pairs. Geochim Cosmochim Acta 58: 2277–2288

Burnham CW, Radoslovich EW (1964) Crystal structures of coexisting muscovite and paragonite. Carnegie Inst Wash, Yearbook 63: 232–236

Busing WR, Levy HA (1964) The effect of thermal motion on the estimation of bond lengths from diffraction measurements. Acta Crystallogr 17: 142–146

Catti M, Ferraris G, Ivaldi G (1988) Thermal behaviour of the crystal structure of strontian piemontite. Am Mineral 73: 1370–1376

Comodi P, Zanazzi PF (1993) Improved calibration curve for the Sm^{2+}: BaFCl pressure sensor. J Appl Cryst 26: 843–845

Comodi P, Zanazzi PF (1995) High-pressure structural study of muscovite. Phys Chem Minerals 22: 170–177

Comodi P, Melacci PT, Polidori G, Zanazzi PF (1994) Trattamento del profilo di diffrazione da campioni in cella ad alta pressione. Proceedings of XXIV National Congress of Associazione Italiana di Cristallografia. Pavia, 27–29 September: 119–120

Denner W, Schulz H, d'Amour H (1978) A new measuring procedure for data collection with a high-pressure cell on X-ray four-circle diffractometer. J Appl Crystallogr 11: 260–264

Finger LW, King H (1978) A revised method of operation of the single-crystal diamond cell and refinement of the structure of NaCl at 32 kbar. Am Mineral 63: 337–342

Guidotti CV (1984) Micas in metamorphic rocks. In: Micas, pp 357–467. Min Soc Am Rev Mineral, vol 13, SW Bailey Ed

Guidotti CV, Sassi FP, Sassi R, Blencoe JG (1994) The effects of ferromagnesian components on the paragonite-muscovite solvus: a semiquantitative analysis based on chemical data for natural paragonite-muscovite pairs. J Metamorphic Geol 12: 779–788

Güven N (1971) The crystal structures of $2M_1$ phengite and $2M_1$ muscovite. Z Kristallogr 134: 196–212

Hazen RM, Finger LW (1982) Comparative crystal chemistry. Wiley, New York

International Tables for X ray Crystallography (1974) Vol IV, Kynoch Press, Birmingham UK

Lin CY, Bailey W (1984) The crystal structure of paragonite $2M_1$. Am Mineral 69: 122–127

North ACT, Phillips DC, Mathews FS (1968) A semiempirical method of absorption correction. Acta Crystallogr A24: 351–359

Radoslovich EW (1963) The cell dimensions and symmetry of layer lattice silicates, IV. Interatomic forces. Am Mineral 48: 76–99

Ross II CR, Webb SL (1990) BIRCH, a program for fitting *PV* data to an Eulerian finite-strain equation of state. J Appl Crystallogr 23: 439–440

Rothbauer R (1971) Untersuchung eines $2M_1$-Muskovits mit Neutronenstrahlen. N Jahrb Mineral Monatsh: 143–154

Sheldrick GM (1976) SHELX-76 Program for crystal structure determination. University of Cambridge, Cambridge UK

Toraya H (1981) Distortions of octahedra and octahedral sheets in 1M micas and the relation to their stability. Z Kristallogr 157: 173–190